The International Journal of Advanced Manufacturing Technology (2018) 99:2035–2044
https://doi.org/10.1007/s00170-018-2646-x

ORIGINAL ARTICLE

Robust design of coordinated decentralized damping controllers for power systems

Murilo E. C. Bento[1] · Daniel Dotta[2] · Roman Kuiava[3] · Rodrigo A. Ramos[1]

Received: 26 June 2018 / Accepted: 26 August 2018 / Published online: 31 August 2018

Abstract

The power system dynamic response is impacted by uncertainties in the system operation such as load variation and large penetration of intermittent generation. This paper presents a method based on the solution of the nonlinear Riccati equation for the design of coordinated robust damping controllers for power systems. The resulting robust controller is of practical application (fixed-order) with a performance guarantee based on quadratic stability. The method is applied to the 68-bus 5-area benchmark test system and the designed controllers are assessed by modal analysis and nonlinear time simulation. The obtained results show better performance of the proposed method compared to benchmark controllers.

Keywords Power system small-signal stability · Oscillatory dynamics damping control · Analytical optimization methods · Uncertainties · Riccati equation

1 Introduction

1.1 Motivation

In the last years, the power system industry is going through important changes with the inclusion of different types of technologies such as intermittent renewable generation (wind and solar photovoltaic), power electronic devices (HVDC, FACTS and storage devices), and intensive use of communication and information technologies tools (PMUs and smart meters). In this scenario, the high intermittent electricity penetration may have negative impacts on a system's stability and reliability as well as other operational issues [4, 18]. The most important consequence is the effect in the inertial response capability of the power system due to a reduction of the system inertia and so affecting its ability to recover frequency and rotor angle stability with respect to large and small disturbances, such as discussed in [22, 24, 29, 31].

The random variations of load, wind, and solar photovoltaic (PV) generation may also introduce uncertainties in the power system operating conditions and so changing how the power system electromechanical modes will evolve turning difficult the design of damping controllers, such as the Power System Stabilizers (PSSs). These difficulties can be offset by several new power electronic devices installed in the power network. These devices, such as HVDC, FACTS, and storage devices even in wind turbines, together with advanced monitoring, such as Wide-Area Measurement Systems (WAMS), can improve the power system's observability and controllability. In this context, the development of methods for the coordinated design of damping controllers with guaranteed robustness in relation to changes in power system parameters is necessary to ensure optimal and reliable system operation [3].

Several methods were proposed in the literature to solve the robust control problem for power systems under different types of uncertainties [10, 12, 19, 21, 25, 30].

This work was financially supported by FAPESP under Grant Nos. 2015/02569-6, 2015/24245-8, 2016/08645-9 and 2018/07375-3.

✉ Murilo E. C. Bento
murilo.bento@usp.br

Daniel Dotta
dottad@unicamp.br

Roman Kuiava
kuiava@eletrica.ufpr.br

Rodrigo A. Ramos
rodrigo.ramos@ieee.org

1 University of Sao Paulo, Av. Trabalhador Sao-Carlense, 400, 13566-590, Sao Carlos, SP, Brazil

2 State University of Campinas, Av. Albert Einstein, 970, 13083-852, Campinas, SP, Brazil

3 Federal University of Parana, Rua Cel. Francisco Heraclito dos Santos, 81531-980, Curitiba, PR, Brazil

Design tools based on Linear Matrix Inequalities (LMIs) [21, 30] and Bilinear Matrix Inequalities (BMIs) [12, 13] techniques were extensively explored because they can guarantee global optimal solution considering uncertainties in the form of linear time-invariant systems in polytopic or norm-bounded domains. The LMI/BMI solvers are based on convex optimization algorithms and it is well known that they are strongly affected by the plant size (dimensionality). The practical results of these limitations are that the current LMI/BMI solvers quickly break down when plants get sizable. Therefore, an usual practice is to adopt model reduction techniques for the control design, but it means controllers without guarantee of stability and performance robustness. In contrast, in the early 2000, the evolution-based search methods were extensively explored because they proved to be able to deal with large dimensional systems [5, 9, 14, 17, 20]. Another recently proposed design method is based on support vector regression [32]. However, these methods present a lack of a formal performance guarantee based on quadratic stability as well as may have a high computational burden.

1.2 Literature review

A deep and relevant literature review and discussion of the main methods and challenges related to damping of electromechanical oscillatory modes are presented in [1, 19]. The authors in [19] proposed a coordination method based on conic programming with promising results. However, the approach does not have a formal proof of stability for all different operating points. Furthermore, the numerical results presented in [19] were performed in the well-known New England New York test system by considering power system stabilizers (PSSs) in all the generators; however, generators 13 to 16 are area-equivalents and PSSs cannot be practically located on these generators.

Several approaches combine LMI/BMI [12, 26, 30] with H_2 and H_∞ minimization [7]. However, they rely on reduced order system and are heavily dependent on weights selection. To tackle these issues, the authors in [1] proposed a fixed-order shaping damping controller design considering parametric uncertainties. The main drawback of the approach is that it is restricted to SISO (Single-Input Single-Output) systems.

The Riccati Lyapunov-based methods are able to deal with large dimensional systems such as presented in [11]. Similar to other Lyapunov-based methods, they are based on a control law that forces the system to descend trajectories around an equilibrium point. Recently, the authors in [33] proposed a control scheme using dynamic stated estimation and an extended linear quadratic regulator (ELQR) to decentralized control design in power systems. The ELQR method proves to have fast convergence and an adequate performance to deal with the design of the proposed control scheme. However, the proposed ELQR is restricted to SISO systems and does not take uncertainties into account.

In [15], the authors present a Riccati Lyapunov-based method to design a centralized damping controller for a two-level control structure. The resulting controller uses phasor measurements from a Wide-Area Measurement System (WAMS) and then time delays were included in the design stage. Although largely explored in literature the centralized control structure is not used in industry. Additionally, the proposed method does not consider uncertainties in the operating condition.

A robust Linear Quadratic Regulator (RLQR) method was proposed by the authors in [6]. This approach includes system uncertainties that must satisfy matching conditions, imposing proper requirements for the choice of weighting matrices. The main disadvantage of this method is that not all types of uncertainties satisfies the necessary matching conditions. In addition, some empirical parameters must also be properly configured and there is not a formal procedure for it. These parameters have a strong potential to affect the method convergence making difficult the application for large power systems.

1.3 Contribution

The paper's main goal is to present a robust design of coordinated fixed-order decentralized damping controllers for power systems. The proposed method is able to deal with high-order power systems, without relying on modal reduction methods. The method also includes parametric uncertainties in the design with stability and performance guarantee resulting on low-order robust controllers. Furthermore, the method presents a simple application and it is not necessary to contrate weights of special parameters that can complicate the control design especially for large power systems.

The method can be applied to different control schemes, such as centralized, quasi-decentralized, and decentralized [15]. The decentralized control scheme is more challenging because of the controllability and observability constraints. This control scheme was also chosen by the recent IEEE benchmark models, which is the basis of comparison [8]. The proposed method presents better results when compared to IEEE benchmark controllers [8]. It should be noted that the benchmark models rely only on conventional generation in a way to properly evaluate the proposed method performance; however, this method can be directly applied for power systems with high penetration of intermittent generation.

The paper is organized as follows. Section 2 presents the power system modeling and control structure. The design method is presented in Section 3. Section 4, describes the application of this method for power system control design. In Section 5, the performance evaluation for the damping controllers designed by the proposed technique is performed via small-signal stability analysis, time-domain nonlinear simulations, and a comparative analysis with the stabilizers originally designed for the two adopted test systems. Section 6 includes the conclusion and final comments.

2 Control problem formulation

A structure based on phase compensation network is adopted in this paper for the PSS-type damping controllers, which is the structure commonly used by the power system industry. The transfer function $dc_i(s)$ for the i^{th} controller (in a total of p controllers) can be written in the Laplace domain as

$$dc_i(s) = \frac{U_i(s)}{Y_i(s)} = \frac{n_3^i s^3 + n_2^i s^2 + n_1^i s + n_0^i}{s^3 + a_2^i s^2 + a_1^i s + a_0^i} \tag{1}$$

$$\equiv \frac{b_2^i s^2 + b_1^i s + b_0^i}{s^3 + a_2^i s^2 + a_1^i s + a_0^i} + d^i \tag{2}$$

$$\equiv K_{dc}^i \cdot \frac{m_3^i s^3 + m_2^i s^2 + m_1^i s + m_0^i}{s^3 + a_2^i s^2 + a_1^i s + a_0^i} \tag{3}$$

where three stages of phase compensation networks are being considered. Also, $U_i(s)$ and $Y_i(s)$ are the Laplace transforms of the output $u_i(t)$ (an additional input signal for the automatic voltage regulator) and the input $y_i(t)$ (generator speed) of the compensator, respectively. The equivalence between (1) and (2) is given by the relations $d^i = n_3^i$, $b_2^i = n_2^i - n_3^i a_2^i$, $b_1^i = n_1^i - n_3^i a_1^i$ and $b_0^i = n_0^i - n_3^i a_0^i$, and the equivalence between (1) and (3) is given by the relations $K_{dc}^i = n_0^i / a_0^i$, $m_0^i = n_0^i / K_{dc}^i = a_0^i$, $m_1^i = n_1^i / K_{dc}^i$, $m_2^i = n_2^i / K_{dc}^i$ and $m_3^i = n_3^i / K_{dc}^i$.

Let us describe the transfer functions $dc_i(s)$, $i = 1, ..., p$, of the damping controllers to be designed in the following form

$$U(s) = \mathbf{DC}(s) Y(s) \tag{4}$$

where $U(s) = [U_1(s) \ \cdots \ U_p(s)]'$, $Y(s) = [Y_1(s) \ \cdots \ Y_p(s)]'$ and $\mathbf{DC}(s)$ is the transfer matrix given by

$$\mathbf{DC}(s) = \begin{bmatrix} dc_1(s) & 0 & \cdots & 0 \\ 0 & dc_2(s) & \cdots & 0 \\ \vdots & \vdots & \ddots & \vdots \\ 0 & 0 & \cdots & dc_p(s) \end{bmatrix} \tag{5}$$

It is important to point out that the block diagonal form in Eq. 5 guarantees the decentralization of the damping controllers, which is a practical requirement of the power system industry. A state-space realization of Eqs. 4–5 can be obtained in the observable canonical form given by

$$\dot{\mathbf{x}}_c = \mathbf{A_c x_c} + \mathbf{B_c y} \tag{6}$$

$$\mathbf{u} = \mathbf{C_c x_c} + \mathbf{D_c y} \tag{7}$$

where $\mathbf{x_c}$, $\mathbf{y}$, and $\mathbf{u}$ are the vectors with, respectively, the states, inputs, and outputs of the controllers in the time domain. Also,

$$\mathbf{A_c} = \begin{bmatrix} \mathbf{A}_{c_1} & \cdots & 0 \\ \vdots & \ddots & \vdots \\ 0 & \cdots & \mathbf{A}_{c_p} \end{bmatrix}, \quad \mathbf{B_c} = \begin{bmatrix} \mathbf{B}_{c_1} & \cdots & 0 \\ \vdots & \ddots & \vdots \\ 0 & \cdots & \mathbf{B}_{c_p} \end{bmatrix}, \tag{8}$$

$$\mathbf{C_c} = \begin{bmatrix} \mathbf{C}_{c_i} & \cdots & 0 \\ \vdots & \ddots & \vdots \\ 0 & \cdots & \mathbf{C}_{c_p} \end{bmatrix}, \text{ and } \mathbf{D_c} = \begin{bmatrix} d^1 & \cdots & 0 \\ \vdots & \ddots & \vdots \\ 0 & \cdots & d^p \end{bmatrix}, \tag{9}$$

where matrices $\mathbf{A}_{c_i}$, $\mathbf{B}_{c_i}$, and $\mathbf{C}_{c_i}$, $i = 1, ..., p$, are given by

$$\mathbf{A}_{c_i} = \begin{bmatrix} 0 & 0 & -a_0^i \\ 1 & 0 & -a_1^i \\ 0 & 1 & -a_2^i \end{bmatrix}, \quad \mathbf{B}_{c_i} = \begin{bmatrix} b_0^i \\ b_1^i \\ b_2^i \end{bmatrix} \tag{10}$$

$$\mathbf{C}_{c_i} = \begin{bmatrix} 0 & 0 & 1 \end{bmatrix} \tag{11}$$

The most widely used techniques for the design of damping controllers for synchronous generators are based on a linear model of the power system in the state-space form given by

$$\dot{\mathbf{x}} = (\mathbf{A} + \Delta\mathbf{A})\mathbf{x} + \mathbf{Bu} \tag{12}$$

$$\mathbf{y} = \mathbf{Cx} \tag{13}$$

where $\mathbf{x} \in \Re^n$ is the state vector. Also, $\mathbf{u} \in \Re^p$ is the vector with the outputs of the damping controllers, which are introduced into the excitation systems at the input to the AVR/exciter and $\mathbf{y} \in \Re^p$ is the vector with the inputs of the damping controllers, which comes from measurements of the power system, such as the rotor speed of the generators. In addition, $\mathbf{A}$, $\mathbf{B}$, and $\mathbf{C}$ are known matrices of adequate dimensions, while $\Delta\mathbf{A}$ is unknown but norm-bounded matrix of an adequate dimension, representing parameter uncertainties.

Now, the closed loop system formed by the interconnection of the power system Eqs. 12–13 with the set of p damping controllers in the state-space form (6)–(7) can be described as

$$\dot{\bar{\mathbf{x}}} = \bar{\mathbf{A}}\bar{\mathbf{x}} \tag{14}$$

where $\bar{\mathbf{x}} = \begin{bmatrix} \mathbf{x} & \mathbf{x_c} \end{bmatrix}^T$ and

$$\bar{\mathbf{A}} = \begin{bmatrix} \mathbf{A} + \mathbf{BD_cC} & \mathbf{BC_c} \\ \mathbf{B_cC} & \mathbf{A_c} \end{bmatrix} \tag{15}$$

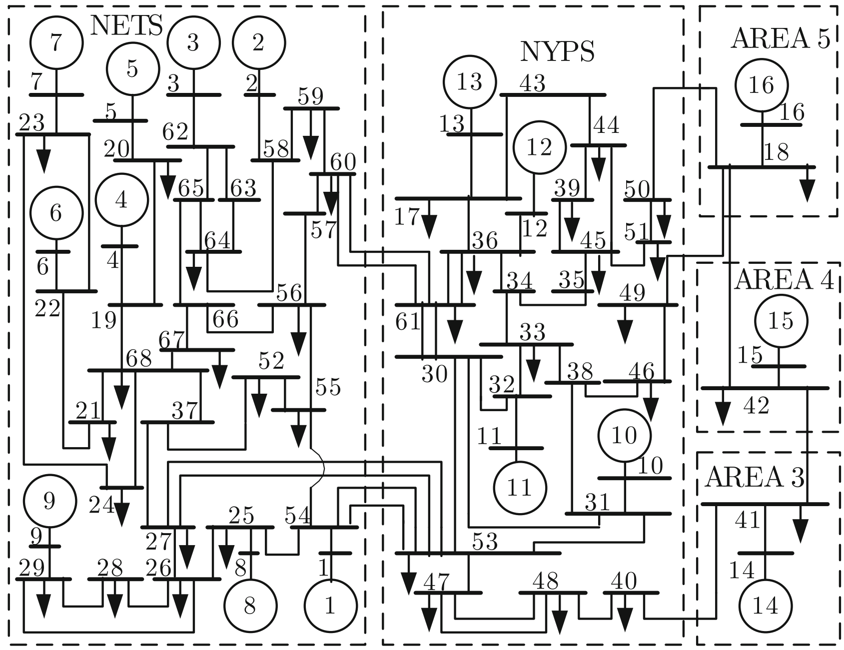

Fig. 1 68-bus test system [8]

Alternatively, by defining the matrices

$$\mathbf{A_a} = \begin{bmatrix} \mathbf{A} & \mathbf{BC_c} \\ \mathbf{0} & \mathbf{A_c} \end{bmatrix}, \quad \mathbf{B_a} = \begin{bmatrix} \mathbf{B} & \mathbf{0} \\ \mathbf{0} & \mathbf{I} \end{bmatrix}, \tag{16}$$

$$\mathbf{C_a} = \begin{bmatrix} \mathbf{C} & \mathbf{0} \end{bmatrix} \tag{17}$$

$$\mathbf{G_a} = \begin{bmatrix} \mathbf{D_c} \\ \mathbf{B_c} \end{bmatrix} \tag{18}$$

and the augmented state vector $\mathbf{x_a} = \begin{bmatrix} \mathbf{x}^T & \mathbf{x_c}^T \end{bmatrix}^T$, an augmented system can be obtained by

$$\dot{\mathbf{x}}_a = \mathbf{A_a x_a} + \mathbf{B_a u_a} \tag{19}$$

$$\mathbf{y_a} = \mathbf{C_a x_a} \tag{20}$$

where the closed loop system given by Eqs. 14–15 is equivalent to the augmented system given by Eqs. 19–20 with the output feedback law given by $\mathbf{u_a} = \mathbf{G_a C_a x_a}$. If the poles of the damping controller are fixed, the parameters a_2^i, a_1^i and a_0^i, $i = 1, \cdots, p$, are previously known, as well as matrices $\mathbf{A_a}$, $\mathbf{B_a}$, and $\mathbf{C_a}$. The control problem of interest is then to determine matrices $\mathbf{D_c}$ and $\mathbf{B_c}$, which corresponds to the gain and zeros of the damping controllers.

3 Methodology

The proposed method aims to find a robust static output feedback controller, through the solution of Algebraic Riccati Equation (ARE). The traditional unconstraint ARE solution, for a known closed loop linear system, presents a unique optimal solution for the state feedback control law given by:

$$\mathbf{u_a} = -\mathbf{K x_a} \tag{21}$$

where $\mathbf{K}$ is the state feedback gain and must satisfy

$$\mathbf{K} = \mathbf{R}^{-1}\mathbf{B_a}^T\mathbf{P} \tag{22}$$

and $\mathbf{P}$ is the solution of ARE:

$$\mathbf{A_a}^T\mathbf{P} + \mathbf{P A_a} - \mathbf{P B_a R}^{-1}\mathbf{B_a}^T\mathbf{P} + \mathbf{Q} = \mathbf{0} \tag{23}$$

The unconstraint problem is well known and can be easily solved with traditional optimization methods. For the sake of power system control system practical design, two structural constraints must be satisfied: output feedback and decentralization.

3.1 Structural constraints

By definition, the decentralization constraint must use only the local states, measured in a specific bus, to feedback a controller installed in the same location. This can be easily implemented by imposing a block diagonal structure on the state feedback matrix. The inclusion of the output feedback constraint is more demanding than decentralization, as described in [16]. In order to fulfill the output feedback constraint, the author in [34] showed in *Lemma 2* that every $\mathbf{K}$ can be written as

$$\mathbf{K} = \mathbf{G_a C_a} - \mathbf{L} \tag{24}$$

where

$$\mathbf{G_a} = (\mathbf{K} + \mathbf{L})\mathbf{C_a}^T(\mathbf{C_a C_a}^T)^{-1} \tag{25}$$

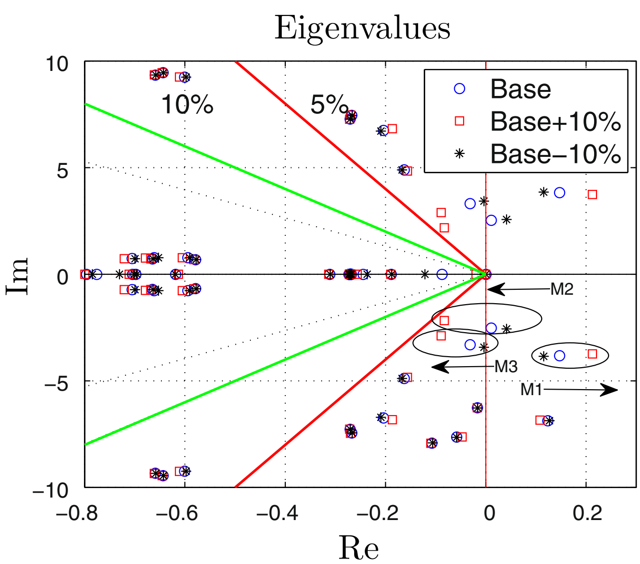

Fig. 2 Eigenvalues for the 68-bus 5-area power system without PSSs

Notice that the calculation of $\mathbf{G_a}$ from Eq. 25 determines the output control law and, consequently, the matrices $\mathbf{D_c}$ and $\mathbf{B_c}$ of the controllers (see Eq. 18).

After the solution of Eq. 23, the matrix $\mathbf{K}$ can be obtained from Eq. 22 and the matrices $\mathbf{G_a}$ and $\mathbf{L}$ in Eq. 24 with the same strategy presented in [34]: using (18), compute the product $\mathbf{G_a C_a}$ and compare to the values between $\mathbf{G_a C_a}$ and $\mathbf{K}$. As a result, the values of $\mathbf{G_a}$ will be automatically obtained since the matrix $\mathbf{C_a}$ is composed by nonzero elements and the remaining values of $\mathbf{K}$.

3.2 Proposed robust design method

The author in [34] proof that a linear uncertain continuous system given by Eqs. 12 and 13 is robust static output feedback stabilizable if:

1. There is a symmetric and positive definite matrix $\mathbf{P} = \mathbf{P}^T > \mathbf{0}$ and a matrix $\mathbf{K}$ if any one of the following conditions is satisfied:

$$[\mathbf{A} + \mathbf{B}(\mathbf{K} + \mathbf{L})]^T \mathbf{P} + \mathbf{P}[\mathbf{A} + \mathbf{B}(\mathbf{K} + \mathbf{L})] + \mathbf{Q_L} < \mathbf{0} \tag{26}$$

where

$$\mathbf{Q_L} = [\Delta\mathbf{A} + \mathbf{B}(\mathbf{K} + \mathbf{L})]^T \mathbf{P} + \mathbf{P}[\Delta\mathbf{A} + \mathbf{B}(\mathbf{K} + \mathbf{L})] \tag{27}$$

2. There exist positive definite matrices $\mathbf{P} = \mathbf{P}^T > \mathbf{0}$ and $\mathbf{R} = \mathbf{R}^T > \mathbf{0}$ and matrices $\mathbf{K}$ and $\mathbf{L}$ satisfying the following matrix inequalities

$$\begin{aligned}&\mathbf{A}^T\mathbf{P} + \mathbf{PA} - \mathbf{PB}\left(\mathbf{R}^{-1} + \mathbf{I}\right)\mathbf{B}^T\mathbf{P} + \mathbf{Q_L} - \\ &\mathbf{K}^T\mathbf{RK} - \mathbf{L}^T\mathbf{L} + (\mathbf{L} + \mathbf{B}^T\mathbf{P})^T(\mathbf{L} + \mathbf{B}^T\mathbf{P}) < \mathbf{0}\end{aligned} \tag{28}$$

$$\left(\mathbf{RK} + \mathbf{B}^T\mathbf{P}\right)^T \phi_L^{-1}\left(\mathbf{RK} + \mathbf{B}^T\mathbf{P}\right) - \mathbf{R} < \mathbf{0} \tag{29}$$

where

$$\begin{aligned}\phi_L = &-[\mathbf{A}^T\mathbf{P} + \mathbf{PA} - \mathbf{PB}\left(\mathbf{R}^{-1} + \mathbf{I}\right)\mathbf{B}^T\mathbf{P} + \mathbf{Q_L} \\ &-\mathbf{K}^T\mathbf{RK} - \mathbf{L}^T\mathbf{L} + (\mathbf{L} + \mathbf{B}^T\mathbf{P})^T(\mathbf{L} + \mathbf{B}^T\mathbf{P})\end{aligned} \tag{30}$$

The author also claims that [34], for the nominal model (12) and (13), an approximate solution $\mathbf{P}, \mathbf{K}$ to the inequalities (28) and (29) is given by these two matrix equalities

$$\mathbf{A}^T\mathbf{P} + \mathbf{PB}(\mathbf{I} + \mathbf{R}^{-1})\mathbf{B}^T\mathbf{P} + \mathbf{Q_{cn}} = \mathbf{0} \tag{31}$$

where

$$\mathbf{Q_{cn}} = (\mathbf{L} + \mathbf{B}^T\mathbf{P})^T(\mathbf{L} + \mathbf{B}^T\mathbf{P}) - \mathbf{L}^T\mathbf{L} - \mathbf{K}^T\mathbf{RK} + \mathbf{Q} \tag{32}$$

and

$$\mathbf{K} = -\mathbf{R^{-1}B^TPC^T}(\mathbf{CC^T})^{-1}\mathbf{y} \tag{33}$$

Based in these assumptions, the following algorithm is proposed [34].

3.3 Algorithm

Step 01: Specify the order and the poles of the controller and, build the matrices $\mathbf{A_c}$ and $\mathbf{C_c}$ in the canonical form such as (8) and (9)

Step 02: Set $i = 1$, $\mathbf{P}_0 = \mathbf{0}$, $\mathbf{L}_0 = \mathbf{0}$, $\mathbf{R_c} = (\mathbf{I} + \mathbf{R}^{-1})^{-1}$ and $\mathbf{Q}_{10} = \mathbf{0}$

Step 03: Compute

$$\begin{aligned}\mathbf{Q}_{\mathbf{c}i} = &\mathbf{Q} + \left[\mathbf{L}_{i-1} + \mathbf{B_a}^T\mathbf{P}_{i-1}\right]^T\left[\mathbf{L}_{i-1} + \mathbf{B_a}^T\mathbf{P}_{i-1}\right] \\ &+\mathbf{Q}_{1(i-1)} - \mathbf{L}_{i-1}^T\mathbf{L}_{i-1} - \mathbf{K}_{i-1}^T\mathbf{RK}_{i-1}\end{aligned} \tag{34}$$

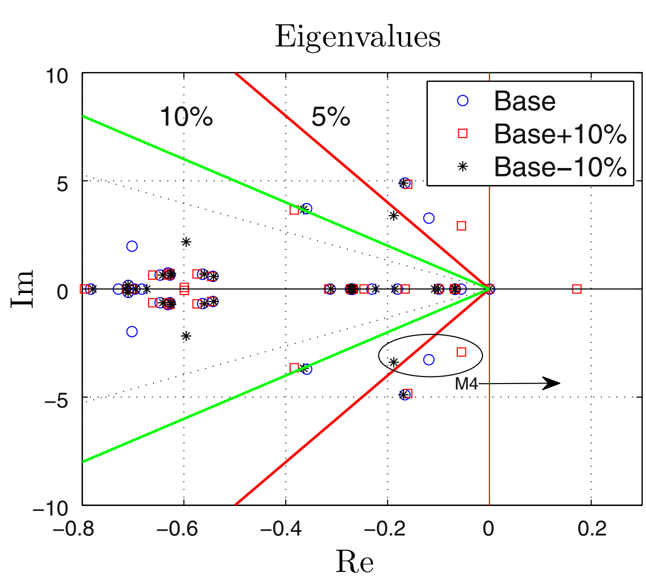

Fig. 3 Eigenvalues for three operating points for the system with the PSSs shown in [8]

Table 1 Parameters of the decentralized controller

dc_n	K_{dc}	m_3	m_2	m_1	m_0	a_2	a_1	a_0
dc_1	11.1104	623.0338	12107.5498	502.3416	15625	75	1875	15625
dc_2	−21.9466	74.4940	183.1893	−189.5205	15625	75	1875	15625
dc_3	−1.4246	619.4720	2404.9658	−8907.5353	15625	75	1875	15625
dc_4	7.3661	734.3461	6948.3362	−5984.9137	15625	75	1875	15625
dc_5	6.7409	−236.1566	−443.7997	−6635.2704	15625	75	1875	15625
dc_6	−1.3684	−4982.8836	−75163.0694	−104280.3777	15625	75	1875	15625
dc_7	3.2645	−257.4835	9427.5892	−976.2775	15625	75	1875	15625
dc_8	8.2253	−55.4991	2068.7985	−11558.7928	15625	75	1875	15625
dc_9	−0.0843	−16784.4280	−82250.9532	−7737780.0436	15625	75	1875	15625
dc_{10}	9.1931	−31.5103	5963.3515	−21085.9658	15625	75	1875	15625
dc_{11}	15.4778	14.9759	1382.1573	382.9916	15625	75	1875	15625
dc_{12}	−8.9352	−412.4180	−11869.8078	−9128.7251	15625	75	1875	15625

Step 04: Solve the ARE:

$$\mathbf{A}_\mathbf{a}^T\mathbf{P}_i + \mathbf{P}_i\mathbf{A}_\mathbf{a} - \mathbf{P}_i\mathbf{B}_\mathbf{a}\mathbf{R}^{-1}\mathbf{B}_\mathbf{a}^T\mathbf{P}_i + \mathbf{Q}_{\mathbf{c}i} = \mathbf{0} \quad (35)$$

where $\mathbf{P}_i = \mathbf{P}_i^T \succ 0$.

Step 05: Compute matrix $\mathbf{K}_i$ as

$$\mathbf{K}_i = -\mathbf{R}^{-1}\mathbf{B}_\mathbf{a}^T\mathbf{P}_i \quad (36)$$

Step 06: For given matrices $\mathbf{K}_i$, $\mathbf{C}_\mathbf{a}$, compute the matrices $\mathbf{G}_{\mathbf{a}i}$ and $\mathbf{L}_i$ based on the strategy presented in Section 3.1.

Step 07: Compute Q_{1i}

$$\mathbf{Q}_{1i} = ||\mathbf{Q}_{Li}||\mathbf{I} = \mathbf{I}\left(\sum_{l=1}^{nu}\epsilon_{lm}||\mathbf{N}_l^T\mathbf{P}_i + \mathbf{P}_i\mathbf{N}_l||\right) \quad (37)$$

where $\epsilon_{lm} = \max|\epsilon_l|$, $l = 1, 2, ..., p$ and

$$\mathbf{N}_l = \mathbf{A}_{\mathbf{a}l} + \mathbf{B}_{\mathbf{a}l}\left(\mathbf{L}_i + \mathbf{K}_i\right) \quad (38)$$

Step 08: Compute $er = ||\mathbf{L}_i - \mathbf{L}_{i-1}||$, if $er \leq tol$ fo to Step 10, otherwise increase i by one and go to Step 3.

Step 09: If there is no solution, change $\mathbf{Q}$ and $\mathbf{R}$ or decrease ϵ_{lm} and go to Step 3.

Step 10: Compute

$$\mathbf{G}_\mathbf{a} = (\mathbf{K}_i + \mathbf{L}_i)\mathbf{C}_\mathbf{a}^T(\mathbf{C}_\mathbf{a}\mathbf{C}_\mathbf{a}^T)^{-1} \quad (39)$$

Step 11: Obtain $\mathbf{B}_\mathbf{c}$ and $\mathbf{D}_\mathbf{c}$ by

$$\mathbf{G}_\mathbf{a} = \begin{bmatrix}\mathbf{D}_\mathbf{c}\\ \mathbf{B}_\mathbf{c}\end{bmatrix} \quad (40)$$

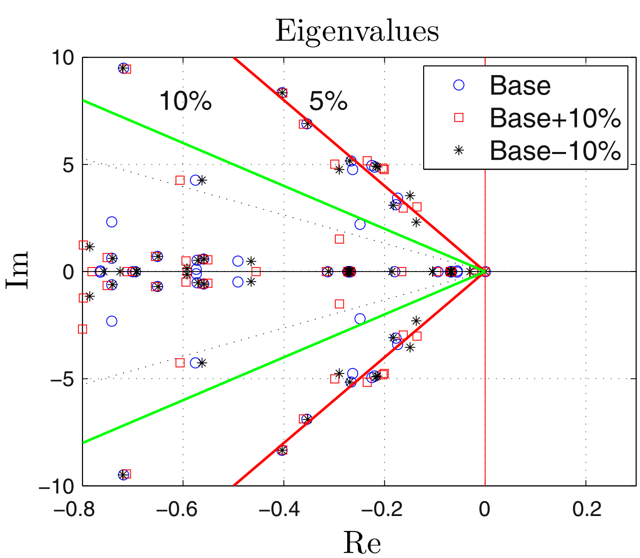

Fig. 4 Eigenvalues for three operating points for the system with the proposed controllers

4 Application to power system damping design

In this section the coordinate controller design main steps will be described as follows:

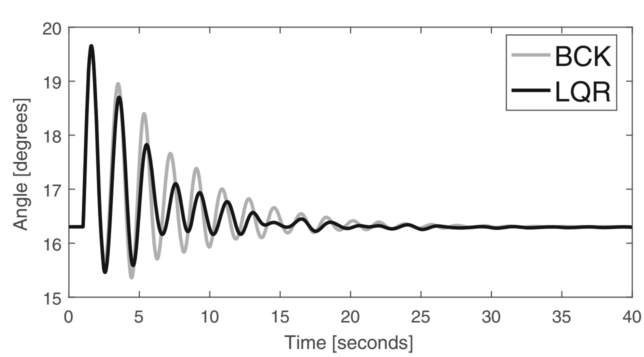

Fig. 5 Rotor angle of the generator 14 for the load case −10%

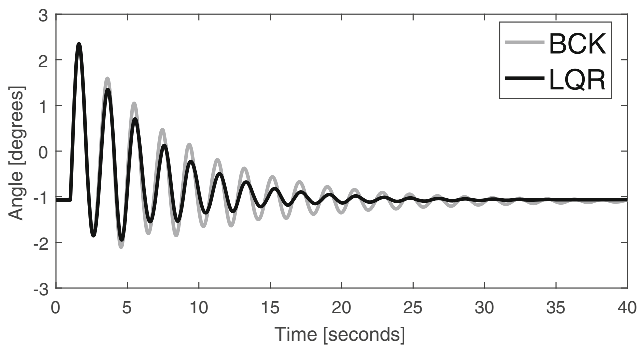

Fig. 6 Rotor angle of the generator 14 for the load base case

1. Weighting matrices: The methods based on Riccati equation or linear quadratic regulator (LQR) are strongly affected by the weighting matrices **Q** and **R**. It is well known that **Q** penalizes the power system states deviations and **R** the input to the excitation system (control effort). The weights for the matrix **Q** are chosen from the selected modes, mainly low damped electromechanical modes, and these are heavily weighted. In this work, the mode shapes, that give an association of state variables and modes, are used to determine the state variables to be weighted for damping a set of oscillation modes. The **R** matrices are weighted when some controller is injecting high magnitude signals that may compromise the control performance.
2. Controller Poles: There is no formal procedure for selecting the poles. In general, the controller coordination main goal is to improve an existent controller configuration. When the manufacturer installs the device, for the utility company, it is already tuned using classical design methods and simplified models (infinity bus machine) [19]. The proposed methodology can be applied for re-tuning the existing stabilizers in the system, aiming at the improvement of the oscillation damping factor under several different operating conditions. In this case, the poles of the controllers can be chosen as the ones of the existing system stabilizers. On the other hand, there is no particular constraint that they must be the same.
3. Uncertainties: In this paper, these matrices were built to cover the entire range of uncertainties of selected operating points. This procedure guarantees that the uncertain closed loop system will be quadratically stable. For the selected operating points all elements are included between the cases of -10% (C1) to $+10\%$ (C2) of load variation w.r.t. the base case. In practice, we set $\mathbf{A}$ equal to the state matrix obtained for the case C1 and $\Delta\mathbf{A}$ is the absolute difference between the elements of the state matrices obtained for the cases C1 and C2. In this work, the parameter ϵ_{lm} is set to be limited between $(-1, +1)$. If the method does not converge ϵ_{lm} can be decreased to reduce the range of the uncertainties.

5 Analysis and numerical simulations

A set of robust controllers was designed for the well-known 68-Bus 5-area power system considering three load levels: a base load, such as specified in [8]; a decrease of “10%” with respect to the base load (C1) and an increment of “10%” of the base load (C2). The section starts with a description of the 68-Bus 5-area power system following the analysis of the controller performance for small-signal and nonlinear time domain simulation perspective. The modal analysis and nonlinear time domain simulations of these three operating conditions were carried out with PacDyn [28] and ANATEM software [2], respectively.

5.1 Test system description

The test system is an equivalent of the interconnected New England and New York power system as shown in Fig. 1 [8]. All the generators are represented by the sixth-order model as well as DC excitation systems (DC4B), except for generator 9 which has a static excitation system ST1A. All the loads are of constant impedance type.

This is the largest benchmark model for small-signal analysis and control presented in [8]. The main challenge is to damp its local and inter-area modes relying only on PSSs, considering that three of its largest machines are system equivalents and not actual power plants. There are four inter-area modes with high participation from the generators 14, 15, and 16. Figure 2 shows the eigenvalues for the three load levels considering the system without PSSs. It can be observed that this system presents three unstable oscillation modes as well as most of the oscillation modes are not affected by the variation in the load conditions.

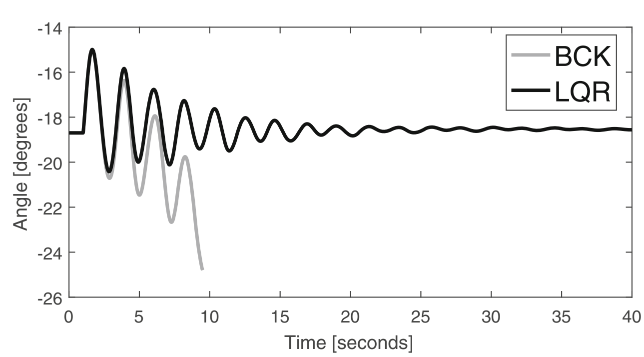

Fig. 7 Rotor angle of the generator 14 for the load case $+10\%$

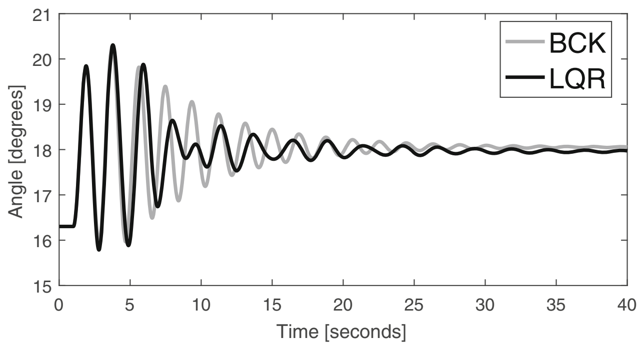

Fig. 8 Rotor angle of the generator 14 for the load case −10%

Three modes are strongly affected by the load conditions and are highlighted in the Fig. 2. Modes 1 (M1) and 2 (M2) are inter-area oscillation modes with high participation of the generator 13. Mode 3 (M3) is a local mode with high participation of the generator 9. These modes are differently affected by the load variation: Mode 1 is strongly impaired by the increase of load; on the other hand, Modes 2 and 3 are strongly impaired by low-load operating points.

This test system was also extensively explored in the literature [8, 19, 27]. Due to the limited number of PSSs installed, some inter-area modes with high participation from generators 13 to 16 may be difficult to damp. Other control schemes using WAMS or FACTS may fix this issue; however, the main goal of this study is to check the method performance in practical situations that do not allow new control schemes or devices (limited controllability and observability conditions). Consequently, following the proposition of [8] only generators 1 to 12 are equipped with PSS devices.

5.2 Small-signal evaluation

The eigenvalues for the three operating conditions considering the system with PSSs designed by the proposed approach are presented in Fig. 4, while Fig. 3 presents the eigenvalues with the PSSs shown in [8]. The authors in [8]

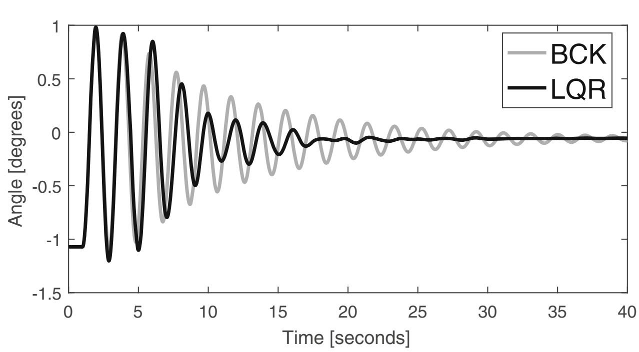

Fig. 9 Rotor angle of the generator 14 for the load base case

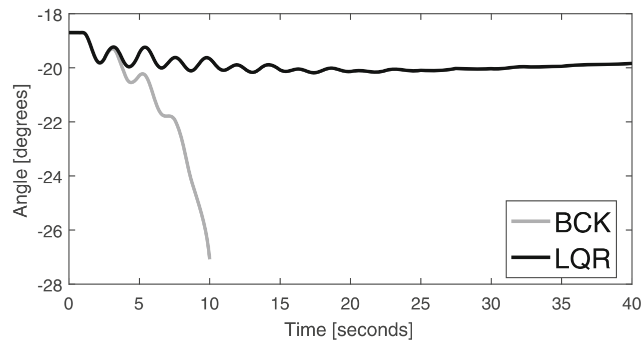

Fig. 10 Rotor angle of the generator 14 for the load case +10%

adopted classical methods for designing the PSSs [23]; however, some inter-area modes remained poorly damped. The controller parameters of the robust control-designed method are presented in Table 1. It can be observed in Fig. 3 that, for the benchmark proposed controllers, the system became unstable with the increase of the load. Additionally, the Mode 4 (M4) related to generator 15 is also impaired by the load increment.

Figure 4 shows that, despite the difficulties to damp several electromechanical modes, the proposed method is able to keep all the eigenvalues close to the suitable minimum damping of 5% for the three load level conditions. The load level variation slightly affects the modes behavior as well as the proposed algorithm guarantee quadratic stability performance for the three conditions.

5.3 Nonlinear time-domain simulations

A nonlinear time-domain simulation was carried out to assess the system performance of the proposed approach (LQR). Two large disturbances were applied: short-circuit and disconnection of a transmission line.

5.3.1 Short-circuit

A 30-ms three-phase short-circuit was applied at bus 14, cleared without any switching. The angle of generator 14 for the three load levels are presented in Figs. 5, 6, and 7. It is clear to see the better damping performance of the controllers designed by the proposed approach (LQR) compared to the performance of the controllers shown in [8] (BCK). The proposed method is also able to keep the power system stable for the load increment case (+10%) as shown in Fig. 7.

5.3.2 Disconnection of a transmission line

This nonlinear simulation includes the contingency given by a permanent disconnection of the transmission line 31–38 in $t = 1$ s. The rotor angle of the generator 14 is presented for the three load levels in Figs. 8, 9, and 10. The simulations results show that the controllers designed by the proposed approach are able to damp out the oscillations faster than the ones shown in [8] in all considered scenarios. The proposed method is also able to keep the power system stable for the load increment case (+10%) as shown in Fig. 10.

6 Conclusions

This paper presented a robust coordination approach for designing decentralized controllers to stabilize multiple oscillation modes. The resulting controller guarantees quadratic stability for the specified range of uncertainties as well as relax the restrictive matching condition specified in [6]. This method can be explored in different control architectures [15] because it proves its satisfactory performance for the challenging decentralized control scheme. Test results in the 68-bus benchmark, with a limited number of PSSs resulting in reduced controllability and observability, show that the method is effective. No model reduction methods were applied in the system and resulting controller. The modal analysis indicates the control robustness for different operating points at a range of uncertainties. Furthermore, a nonlinear simulation performed verifies the presented method concept and the designed decentralized controller under various operating conditions.

Acknowledgements The authors gratefully acknowledge the permission of CEPEL for the use of ANATEM and PacDyn and Prof. Aguinaldo S. e Silva for carefully reading our paper.

Publisher's Note Springer Nature remains neutral with regard to jurisdictional claims in published maps and institutional affiliations.

References

1. Abdlrahem AA, Hadidi R, Karimi A, Saraf P, Makram E (2017) Fixed-order loop shaping robust controller design for parametric models to damp inter-area oscillations. Int J Electr Power Energy Syst 88:164–174. https://doi.org/10.1016/j.ijepes.2016.12.013
2. ANATEM (2014) Anatem user's manual version 10.5.2. CEPEL Available: http://www.dre.cepel.br/
3. Annaswamy AM, Amin M (2013) IEEE vision for smart grid controls: 2030 and beyond, 1–168
4. Ayodele TR, Jimoh AA, Munda JL, Agee JT (2012) Challenges of grid integration of wind power on power system grid integrity: a review. Int J Renew Energy Res 2(4):815–824
5. Bento MEC, Dotta D, Kuiava R, Ramos RA (2018) A procedure to design fault-tolerant wide-area damping controllers. IEEE Access 6:23,383–23,405. https://doi.org/10.1109/ACCESS.2018.2828609
6. Bento MEC, Dotta D, Kuiava R, Ramos RA (2018) Design of coordinated decentralized damping controllers for power systems considering uncertainties. J Control Autom Electric Syst 29(1):22–31. https://doi.org/10.1007/s40313-017-0351-x
7. Boukarim GE, Wang S, Chow JH, Taranto GN, Martins N (2000) A comparison of classical, robust, and decentralized control designs for multiple power system stabilizers. IEEE Trans Power Syst 15(4):1287–1292. https://doi.org/10.1109/59.898103
8. Canizares C, Fernandes T, Geraldi E, Gerin-Lajoie L, Gibbard M, Hiskens TF, Past Chair I, Kersulis J, Kuiava R, Lima L, DeMarco F, Martins N, Pal BC, Piardi A, Ramos TF, Chair R, dos Santos J, Silva D, Singh AK, Tamimi B, Vowles D (2017) Benchmark models for the analysis and control of small-signal oscillatory dynamics in power systems. IEEE Trans Power Syst 32(1):715–722. https://doi.org/10.1109/TPWRS.2016.2561263
9. Castoldi MF, Sanches DS, Mansour MR, Bretas NG, Ramos RA (2014) A hybrid algorithm to tune power oscillation dampers for FACTS devices in power systems. Control Eng Pract 24:25–32. https://doi.org/10.1016/j.conengprac.2013.11.001
10. Chaudhuri B, Pal BC, Zolotas AC, Jaimoukha IM, Green TC (2003) Mixed-sensitivity approach to Hinfty control of power system oscillations employing multiple facts devices. IEEE Trans Power Syst 18(3):1149–1156. https://doi.org/10.1109/TPWRS.2003.811311
11. Costa AJAS, Freitas FD, e Silva AS (1997) Design of decentralized controllers for large power systems considering sparsity. IEEE Trans Power Syst 12(1):144–152. https://doi.org/10.1109/59.574934
12. Deng J, Zhang XP (2014) Robust damping control of power systems with TCSC: a multi-model BMI approach with H2 performance. IEEE Trans Power Syst 29(4):1512–1521. https://doi.org/10.1109/TPWRS.2013.2292067
13. Deng J, Li C, Zhang XP (2015) Coordinated design of multiple robust FACTS damping controllers: a BMI-based sequential approach with multi-model systems. IEEE Trans Power Syst 30(6):3150–3159. https://doi.org/10.1109/TPWRS.2015.2392153
14. Do Bomfim ALB, Taranto GN, Falcao DM (2000) Simultaneous tuning of power system damping controllers using genetic algorithms. IEEE Trans Power Syst 15(1):163–169. https://doi.org/10.1109/59.852116
15. Dotta D, e Silva AS, Decker IC (2009) Wide-area measurements-based two-level control design considering signal transmission delay. IEEE Trans Power Syst 24(1):208–216. https://doi.org/10.1109/TPWRS.2008.2004733
16. Geromel JC, Peres PLD (1985) Decentralised load-frequency control. IEE Proc D Control Theory Appl 132(5):225–230. https://doi.org/10.1049/ip-d.1985.0039
17. Guesmi T, Farah A, Abdallah HH, Ouali A (2018) Robust design of multimachine power system stabilizers based on improved non-dominated sorting genetic algorithms. Electr Eng 100(3):1351–1363. https://doi.org/10.1007/s00202-017-0589-0
18. Ibrahim H, Ghandour M, Dimitrova M, Ilinca A, Perron J (2011) Integration of wind energy into electricity systems: technical challenges and actual solutions. Energy Procedia 6:815–824. https://doi.org/10.1016/j.egypro.2011.05.092
19. Jabr RA, Pal BC, Martins N (2010) A sequential conic programming approach for the coordinated and robust design of power system stabilizers. IEEE Trans Power Syst 25(3):1627–1637. https://doi.org/10.1109/TPWRS.2010.2040637
20. Jebali M, Kahouli O, Hadj Abdallah H (2017) Optimizing PSS parameters for a multi-machine power system using genetic algorithm and neural network techniques. Int J Adv Manuf Technol 90(9-12):2669–2688. https://doi.org/10.1007/s00170-016-9547-7
21. Kuiava R, Ramos RA, Pota HR (2013) A new method to design robust power oscillation dampers for distributed synchronous generation systems. J Dyn Syst Measur Control 135(3):031,011. https://doi.org/10.1115/1.4023225
22. Lara-Jimenez JD, Ramrez JM, Mancilla-David F (2017) Allocation of PMUs for power system-wide inertial frequency

response estimation. IET Gen Trans Distrib 11(11):2902–2911. https://doi.org/10.1049/iet-gtd.2016.1951

23. Larsen EV, Swann DA (1981) Applying power system stabilizers Part I: basic concepts. IEEE Trans Power Apparatus Syst PAS-100 n(6):3017–3024. https://doi.org/10.1109/TPAS.1981.316355
24. Lugnani L, Dotta D, Decker IC, Chow JH (2018) Frequency response estimation following large disturbances using synchrophasors. In: 2018 IEEE Power & energy society general meeting, pp 1–5. IEEE
25. Majumder R, Pal BC, Dufour C, Korba P (2006) Design and real-time implementation of robust FACTS controller for damping inter-area oscillation. IEEE Trans Power Syst 21(2):809–816. https://doi.org/10.1109/TPWRS.2006.873020
26. Bento MEC, Kuiava R, Ramos RA (2018) Design of wide-area damping controllers incorporating resiliency to permanent failure of remote communication links. J Control Autom Electr Syst 29(5):541–550. https://doi.org/10.1007/s40313-018-0398-3
27. Oliveira RV, Kuiava R, Ramos RA, Bretas NG (2009) Automatic tuning method for the design of supplementary damping controllers for flexible alternating current transmission system devices. IET Gen Trans Distrib 3(10):919–929. https://doi.org/10.1049/iet-gtd.2008.0424
28. PACDYN (2015) PacDyn documentation. CEPEL Available: http://www.pacdyn.cepel.br
29. Rahmann C, Castillo A (2014) Fast frequency response capability of photovoltaic power plants: the necessity of new grid requirements and definitions. Energies 7(10):6306–6322. https://doi.org/10.3390/en7106306
30. Ramos RA, Alberto LFC, Bretas NG (2004) A new methodology for the coordinated design of robust decentralized power system damping controllers. IEEE Trans Power Syst 19(1):444–454. https://doi.org/10.1109/TPWRS.2003.820690
31. Ruttledge L, Flynn D (2011) System-wide inertial response from fixed speed and variable speed wind turbines. In: 2011 IEEE Power and energy society general meeting. IEEE, pp 1–7. https://doi.org/10.1109/PES.2011.6038883
32. Shahriar MS, Shafiullah M, Rana MJ (2018) Stability enhancement of PSS-UPFC installed power system by support vector regression. Electr Eng 100(3):1601–1612. https://doi.org/10.1007/s00202-017-0638-8
33. Singh AK, Pal BC (2016) Decentralized control of oscillatory dynamics in power systems using an extended LQR. IEEE Trans Power Syst 31(3):1715–1728. https://doi.org/10.1109/TPWRS.2015.2461664
34. Veselý V (2002) Robust output feedback controller design for linear parametric uncertain systems. J Electr Eng 53(5):117–125